

*Original Article*

## **Klotho reduces apoptosis in experimental ischaemic acute renal failure**

Hidekazu Sugiura<sup>1</sup>, Takumi Yoshida<sup>1,2</sup>, Ken Tsuchiya<sup>1</sup>, Michihiro Mitobe<sup>1</sup>, Sayoko Nishimura<sup>1</sup>, Satsuki Shirota<sup>1</sup>, Takashi Akiba<sup>1,2</sup> and Hiroshi Nihei<sup>1</sup>

<sup>1</sup>Department of Medicine IV and <sup>2</sup>Department of Blood Purification, Tokyo Women's Medical University, Tokyo, Japan

### **Abstract**

**Background.** Klotho is associated with the suppression of several ageing phenotypes. Because high klotho gene expression was detected in the kidney and several studies have found altered expression in animal models, we explored the physiological relevance of klotho expression in the kidney under renal ischemia reperfusion injury (IRI).

**Methods.** Male Wistar rats were subjected to bilateral renal ischemia or sham operation, followed by reperfusion for 6, 12 or 24 h, or 2 to 10 days. Renal expression of klotho was assessed by real-time PCR or Western blotting. Creatinine levels were determined. Immunohistochemical studies and TUNEL staining were performed. An adenovirus harbouring the mouse klotho gene (ad-kl) was intravenously administered to one group of rats before renal IRI.

**Results.** Renal klotho mRNA and protein expressions were significantly reduced in IRI rats the first day after ischemia. Pre-treatment with ad-kl resulted in a robust induction of klotho mRNA and protein in the liver but not in the kidney. Ad-kl gene transfer improved serum creatinine and the histological changes. Apoptosis induced by IRI was attenuated following ad-kl administration.

**Conclusion.** The data suggest klotho to be involved in the pathophysiology of IRI. Downregulation of renal klotho exacerbates ischaemic acute renal failure, and klotho gene induction has therapeutic potential in managing ischaemic renal damage.

**Keywords:** adenovirus; apoptosis; ischemia reperfusion; klotho

### **Introduction**

Klotho gene expression defects in the mouse result in a syndrome that resembles human ageing, including a shortened lifespan, infertility, arteriosclerosis, mitral annular calcification, skin atrophy, osteoporosis, and emphysema [1]. The klotho gene is expressed predominantly in the kidney and choroid plexus, with little if any expression in other organs [1]. A splice variant of klotho mRNA, encoding a putative secreted protein, was identified [2]. However, the precise regulation and significance of klotho expression have not yet been clarified. Recent studies have shown klotho expression to be suppressed in several animal models under sustained stress conditions [3]. Moreover, renal expression of the klotho gene was reported to be markedly suppressed in chronic renal failure patients [4]. All these reports suggest that stressful conditions downregulate klotho expression, resulting in cell or organ dysfunction resembling age-related complications.

Thus, in the present study, we adopted the stress-induced kidney injury model, i.e. renal ischemia-reperfusion injury (IRI), to investigate the regulatory mechanism of klotho expression in the kidney. It has been established that oxidative stress is involved in renal IRI leading to tissue damage and dysfunction. In addition to the increase in reactive oxygen species, inflammation is involved in this process [5], resulting in cell necrosis and apoptosis as in ARF [6]. Moreover, to clarify the possible physiological role of the klotho gene in this model, an exogenous klotho gene was transfected into an animal model, and functional and histological changes in the kidney were analysed.

### **Methods**

#### *Experimental animal model*

*In vivo* studies were carried out using 150 male Wistar rats weighing 200 to 250 g (7–8 weeks old), with free access to

Correspondence and offprint requests to: Takumi Yoshida, MD, PhD, Department of Blood Purification, Tokyo Women's Medical University, 8-1 Kawada-cho, Shinjuku-city, Tokyo 162-8666, Japan. Email: tyoshida@kc.twmu.ac.jp

standard food and water, cared for in accordance with the Institutional Animal Research Committee *Guide for the Care and Use of Laboratory Animals* published by the US National Institutes of Health (NIH publication number 85–23, revised 1996). Animals undergoing operations were anesthetized with pentobarbiturate. Animals were randomly divided into the following three groups.

- (1) Renal IRI group. The renal ischemia-reperfusion model was produced as previously reported [7]. Briefly, under anaesthesia, the bilateral renal arteries and veins were exposed using an abdominal central incision, and the renal pedicles were clamped with arterial clips for 60 min. Ischaemic kidneys were reperfused for 6, 12 or 24 h, or for 2 to 6 or 10 days ( $n=6-8$ ).
- (2) Sham group. Under anaesthesia, the bilateral renal arteries and veins were exposed using a central abdominal incision, but these rats did not undergo bilateral renal clamping. Non-ischaemic kidneys were followed using the same protocol as above ( $n=6-8$ ).
- (3) Control group. In this group, rats were neither anesthetized nor operated on ( $n=6-8$ ).

After the stated times, the animals were painlessly killed, blood samples were collected and both kidneys and the liver were removed. The kidneys were quartered, two of the kidney specimens were then snap-frozen in liquid nitrogen, and the remaining specimens were fixed with either 15% neutral buffered formalin or 4% paraformaldehyde in phosphate-buffered saline (PBS). Two hepatic specimens were snap-frozen in liquid nitrogen.

#### *Measurement of biochemical parameters*

The blood samples were centrifuged (5000 r.p.m. for 10 min) to separate the plasma. Plasma concentrations of creatinine (PCr) were measured with an auto-analyser (SRL, Tokyo, Japan) as indicators of impaired glomerular function.

#### *RNA isolation, reverse transcription (RT), and real time PCR*

This assay was performed as previously described [7]. Total RNA was extracted from the kidney and liver using TRIZOL (Invitrogen, Tokyo, Japan). cDNA was then prepared with a Super Script kit (Invitrogen, Tokyo, Japan) from 5 µg total RNA with Oligo (dT) for analysis by real time PCR using Prism 7700 (Applied Biosystems, Sequence Detection Systems 1.6.3, Tokyo, Japan) with klotho specific primers (5' CGT GAA TGA GGC TCT GAA AGC 3' (forward) and 5' GAG CGG TCA CTA AGC GAA TAC G 3' (reverse)), and finally normalized with rat glyceraldehyde-3-phosphate dehydrogenase (GAPDH) (Rodent, Tokyo, Japan) cDNA. The exogenous expression of mouse klotho mRNA was detected by real time PCR with primers 5' CAA AGT CTT CGG CCT TGT TC 3' (forward) and 5' CTC CCC AAG CAA AGT CAC A 3' (reverse) primers.

#### *Western blotting*

Frozen kidney and liver specimens were immersed in a lysis buffer (20 mM Tris buffer, pH 7.5, containing 1 mM phenylmethylsulfonyl fluoride, 10 µg/ml aprotinin from

bovine lung (Wako, Tokyo, Japan), 2 mM DL-dithiothreitol, 1% polyoxyethylene sorbitan monolaurate, 1 mM ethylenediamine tetraacetate), homogenized on ice and centrifuged at 5000 r.p.m. for 10 min then, 300 µg of protein from each sample were suspended in a loading buffer, separated on a 10% polyacrylamide gel (Readygels J, BIO-RAD, Tokyo, Japan), and electrophoretically transferred to a nitrocellulose membrane. Membranes were blocked with 3% skimmed milk overnight at 4°C. A monoclonal antibody against the recombinant human klotho protein, KM2076 [8] (generously provided by Kyowa Hakko Kogyo, Shizuoka, Japan), was used at a 1:3000 dilution. The primary antibody was applied overnight at 4°C. After two 10 min washing steps with washing buffer (0.3% Tween20 in PBS), the membrane was incubated with horseradish peroxidase-conjugated rabbit anti-rat immunoglobulins (DAKO, Tokyo, Japan) for 1 h at room temperature. The membrane was incubated with an ECL Western blotting system (Amersham Biosciences, Tokyo) and then exposed to X-ray film. Quantification was performed with relative density employing Image J, an image processing program.

#### *Frozen immunohistochemical analysis*

Kidneys were fixed with 4% paraformaldehyde in PBS for 16 h at 4°C, immersed sequentially in 10%, 15% and then 20% sucrose in PBS for 12 h at 4°C, embedded in OCT compound and immediately frozen in liquid nitrogen. Immunohistochemical analysis was performed with a primary antibody against the recombinant human klotho protein, KM2076, and a secondary antibody (Alexa Fluor 488 goat anti-rat IgG (H+L), Molecular Probes, Tokyo, Japan). Nonspecific binding sites were blocked in 3 µm sections with goat serum (Gibco, Tokyo, Japan) (10% goat serum, 20 mM Tris, 225 mM NaCl, 1% BSA) for 1 h at room temperature, and blocked with anti-rat IgG (Anti-rat IgG(H+L), Vector Laboratories, Tokyo, Japan) for 3 h with TBS (20 mM Tris, 225 mM NaCl), then incubated with the primary antibody, diluted 1:300, for 16 h at 4°C. After three 5 min washing steps with TBS, the sections were incubated with the secondary antibody diluted 1:200, for 1 h at room temperature in the dark. After three 5 min washing steps with TBS, the sections were mounted using VectaShield (Vector Laboratories, Tokyo, Japan).

#### *Paraffin immunohistochemical analysis*

The kidneys were fixed with 4% paraformaldehyde in PBS for 16 h at 4°C, and then embedded in paraffin. Three micron paraffin sections were deparaffinized and hydrated. The sections were incubated for 30 min in 0.3% H<sub>2</sub>O<sub>2</sub> in methanol. We used a Vectastain ABC Kit Rat IgG (Vector Laboratories, Tokyo, Japan) for immunohistochemical staining. Sections were primarily blocked with rabbit serum (20 mM Tris, 225 mM NaCl, 0.15% rabbit serum) for 20 min, then with anti-rat IgG for 15 min, and incubated with the primary antibody against the recombinant human klotho protein, KM2076, for 30 min. After incubation with the biotinylated secondary antibody solution for 30 min, the sections were incubated with Vectastain ABC Reagent for 30 min, and incubated with a peroxidase substrate solution DAB substrate kit (Vector Laboratories, Tokyo, Japan).

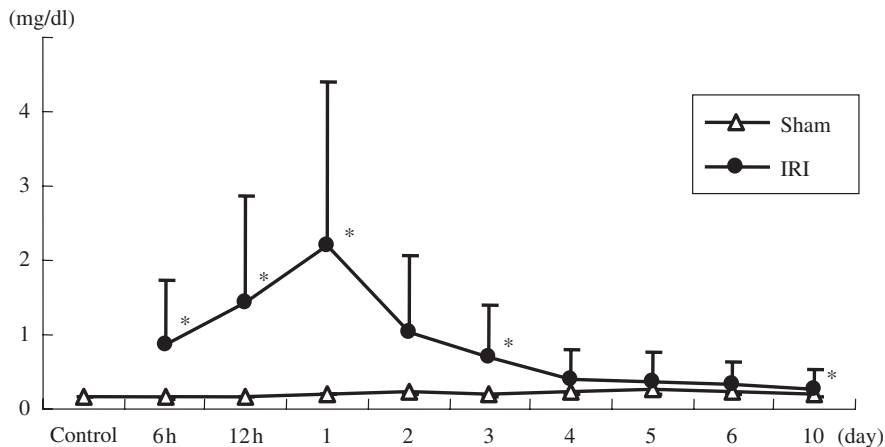


**Fig. 1.** Plasma concentrations of creatinine. Creatinine was significantly elevated in IRI rats. Data are given as means  $\pm$  SD. \* $P < 0.01$  compared with sham-operated rats. ( $n = 6$  to 8 for control, 6 h, 12 h, 1 day, 3 day and 10 day groups.  $n = 3$  for other groups.)

#### Detection of apoptotic cells—terminal deoxyribonucleotide transferase (TdT)-mediated dUTP nick-end labelling (TUNEL) stain

The TUNEL procedure was applied to the renal sections to determine DNA fragmentation as an index of apoptosis. Counterstaining was performed using 4',6-diamidino-2'-phenylindole dihydrochloride (DAPI) dye (1  $\mu$ g/ml, Kirkegaard Perry Laboratories, Tokyo, Japan). Frozen 3  $\mu$ m sections, fixed with 4% paraformaldehyde in PBS, were stained using an *in situ* cell death detection kit, TMR red (Roche, Tokyo, Japan). Kidney sections were incubated in permeabilization solution (0.1% Triton X-100 in 0.1% sodium citrate) for 2 min on ice. After rinsing twice with PBS, the samples were incubated with TUNEL reaction mixture for 60 min at 37°C in the dark. After being rinsed twice with PBS, samples were incubated with DAPI dye, diluted 1:1000, for 4 min in the dark. Finally, the sections were mounted using VectaShield.

#### Histological examinations

The kidneys were fixed with 15% neutral buffered formalin, and then embedded in paraffin. For morphologic evaluations, 3  $\mu$ m paraffin sections were routinely stained with hematoxylin–eosin (HE) and periodic acid–Schiff (PAS). Histological examinations were performed by three renal pathologists in a blinded fashion [9]. Histological changes due to tubular necrosis were quantified by calculation of the percentage of tubules displaying cellular necrosis, loss of the brush border, cast formation, and tubule dilatation, as follows: 0, none; 1, 10%; 2, 11–25%; 3, 26–45%; 4, 46–75%; and 5, >76%. At least fifteen fields ( $\times 200$ ) were reviewed for each slide in the HE-stained specimens (ATN score).

Apoptotic cells (TUNEL-positive cells) were quantitatively assessed per 10 high-power fields ( $\times 400$ ) by the renal pathologists in a blinded fashion in the TUNEL stained specimens.

#### Construction of recombinant adenoviruses and adenovirus-mediated transfer

An adenovirus encoding the mouse *klotho* gene (ad-kl) (generously provided by Kyowa Hakko Kogyo, Shizuoka,

Japan) was constructed using cosmid cassettes and the adenovirus DNA-terminal protein complex (COS-TPC) method as described elsewhere [10]. An adenovirus harbouring the *Escherichia coli*  $\beta$ -galactosidase gene was designated ad-LacZ. Vectors were purified using two consecutive CsCl gradient ultracentrifugations, dialyzed at 4°C against a sterile virus buffer, and stored at  $-80^\circ\text{C}$  until use. Recombinant adenovirus was titred using 293 cells, by the Tissue Culture Infections Dose 50 Method (TCID50). TCID50 assays were done at least twice, always including the same ad-LacZ viral preparation as the standard control.

Purified recombinant *klotho* adenovirus was injected into rats through the tail vein at a dose of  $1.6 \times 10^{10}$  plaque forming units (pfu). The same ischaemic procedure was carried out 3 days after the gene transfer. Ischaemic kidneys were analysed for 72 h. Tail vein blood samples (0.2 ml) were obtained for 1, 3, 5, 7 days. The data were compared with those of the ad-LacZ and sham-operated groups.

#### Statistical analysis

Data are presented as means  $\pm$  SD. Statistical analysis was performed with Excel for Windows. The unpaired *t*-test was used. Values of  $P < 0.05$  were considered significant.

## Results

#### IRI downregulated renal expression of *klotho* mRNA and protein

PCr was significantly elevated in IRI rats as compared with sham rats at the first day after the operation (day 1: IRI;  $2.19 \pm 1.03$  mg/dl vs sham;  $0.21 \pm 0.025$  mg/dl,  $P < 0.001$ ). Subsequently, PCr improved in a time-dependent manner, but had not returned to the normal range by 10 days after the operation (day 10: IRI;  $0.27 \pm 0.017$  mg/dl vs sham;  $0.20 \pm 0.045$  mg/dl,  $P < 0.01$ ) (Figure 1). The PCr values of sham group rats were the same as those of the control group.

Expression of *klotho* mRNA was significantly reduced in the IRI kidney, but gradually rose to

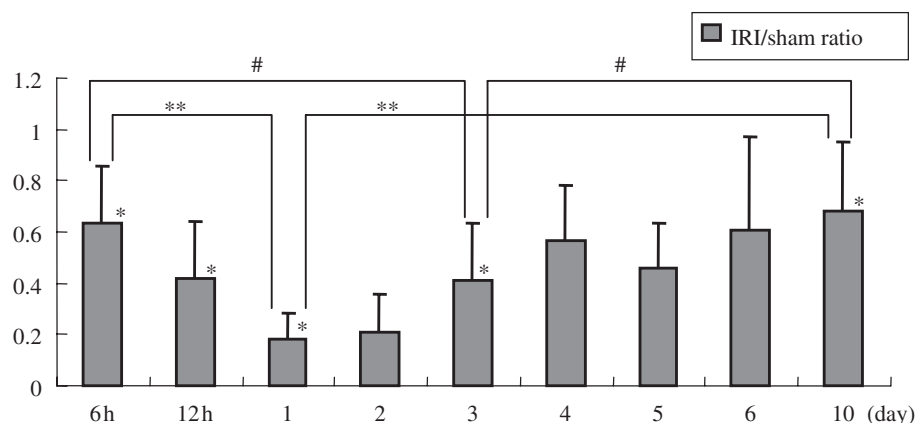


**Fig. 2.** Klotho mRNA expression in the kidney after IRI operation (the ratios of mRNA expression in IRI/sham). Renal klotho mRNA expression was significantly reduced in IRI rats. Data are given as means  $\pm$  SD. # $P < 0.05$  compared with day 3, \*\* $P < 0.01$  compared with day 1, \* $P < 0.01$  compared with sham-operated rats. ( $n = 6$  to 8 for control, 6h, 12h, 1 day, 3 day, and 10 day groups.  $n = 3$  for other groups.)

nearly the control level. The klotho mRNA level of rats 10 days after renal IRI was still reduced in comparison with that of sham-operated rats (Figure 2). The klotho mRNA levels of sham group rats were the same as those of the control group (data not shown).

Representative protein expression blotting is shown in Figure 3a. Initially reduced expression gradually normalized after ischemia. Relative expression in arbitrary units is shown in Figure 3b, and klotho protein expression was significantly reduced in the IRI group on the first day after ischemia. Klotho protein expression subsequently improved in a time-dependent manner.

IRI severely damaged tubules, with loss of the brush border, detachment of epithelial cells from the basement membrane and tubular obstruction on the first day, then tubular dilatation at 3 to 10 days, as shown by the HE staining. The rats that underwent the sham operation exhibited no abnormalities (Figure 4a). There was no glomerular damage in either the IRI or the sham-operated groups, as demonstrated by PAS staining (data not shown). Immunohistological staining revealed klotho protein in the sham group to be predominantly expressed in distal tubular epithelial cells of the cortex and medulla (Figure 4). Klotho staining was reduced on the first day after IRI in these regions, but the staining intensity showed slight recovery 10 days after ischemia. Representative staining of paraffin sections is shown in Figure 4b, illustrating the orientation of klotho expression localization.

#### Relation between klotho expression and apoptosis in renal ischaemic injury

Tissue damage was so severe that there were no detectable klotho positive cells and TUNEL staining was prominent in cells detached from the basement membrane on the first day (data not shown). Following the time course of histological changes, the number of klotho positive cells in the kidney 3 days after IRI was less than that in the sham-operated kidney. In addition,

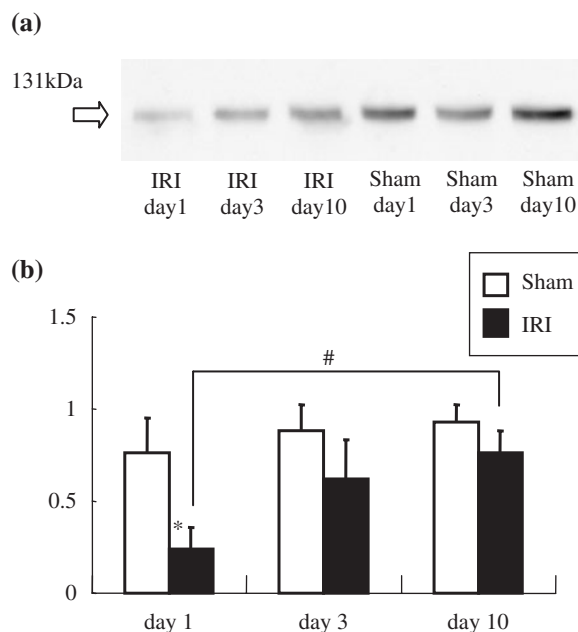
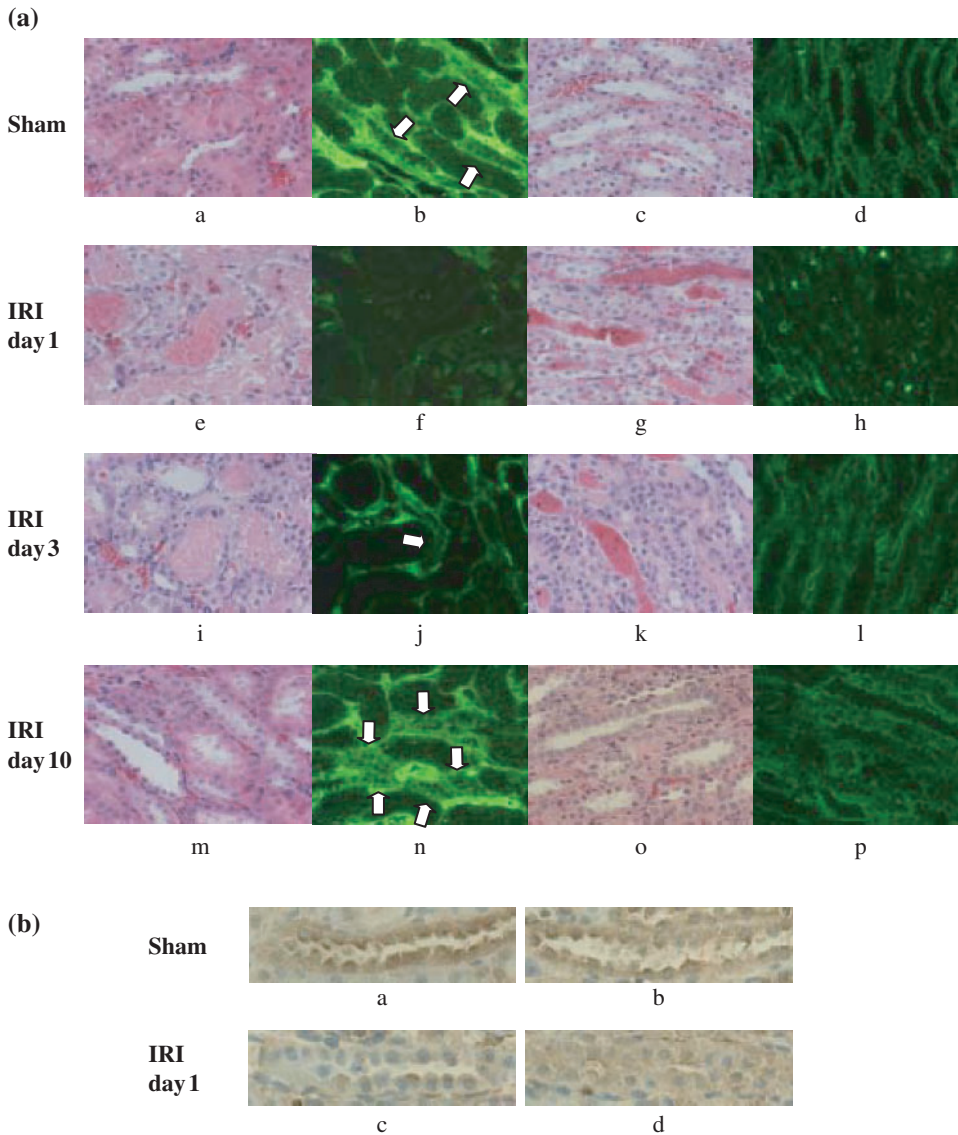


**Fig. 3.** Klotho protein expression in the kidney after IRI operation. (a) Representative Western blotting. (b) Summary of the Western blot data. Klotho protein expression was significantly reduced in IRI rats at day 1. Data are given as means  $\pm$  SD. \* $P < 0.01$  compared with sham operated-rats. # $P < 0.05$  compared with day 10. ( $n = 4$  for each group.)

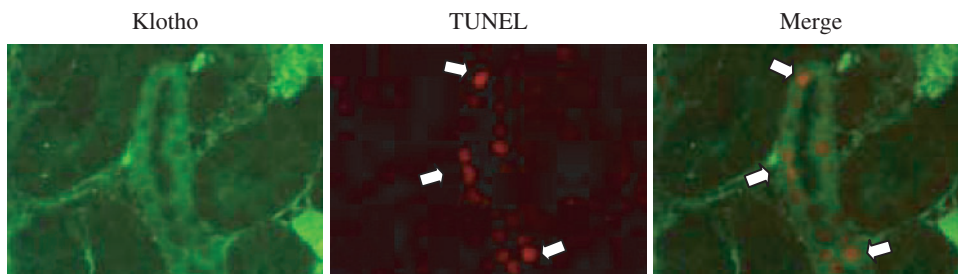
3 days after IRI, there were some TUNEL-positive cells in renal tubules in which cells stained positively for klotho (Figure 5). Typically, TUNEL-positive cells were positively co-stained with klotho in tubules. The number of TUNEL-positive cells decreased over time (data not shown).

#### Effects of klotho gene transfer on IRI renal injury

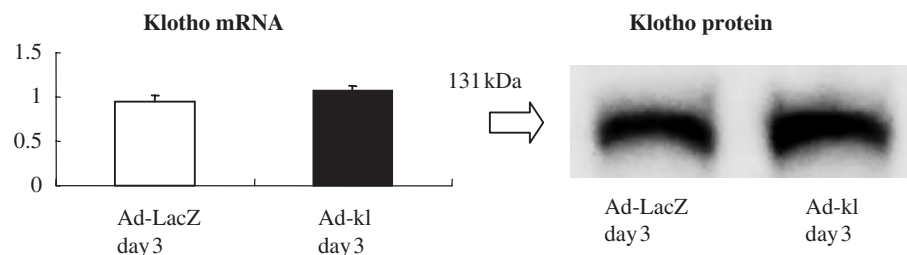
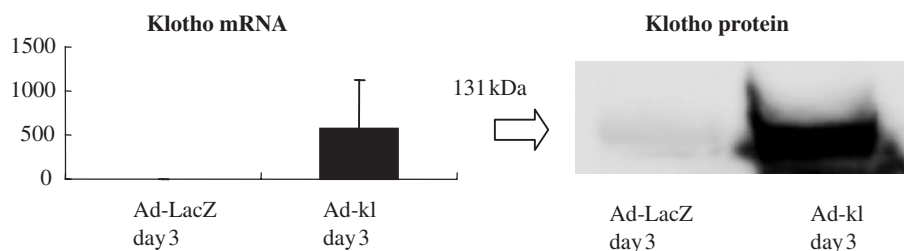
Either ad-kl or ad-LacZ at a dose of  $1.6 \times 10^{10}$  pfu was intravenously administered to rats 3 days before the IRI procedure. Three days after administration,



**Fig. 4.** Representative immunohistochemical staining shows klotho expression in renal tubules. Sections for immunohistochemistry are presented with HE-stained paraffin sections for orientation. **(a)** The staining intensity was significantly reduced in IRI rats at day 1. The intensity was apparently improved at day 10. a–d; Sham, e–h; IRI day 1, i–l; IRI day 3, m–p; IRI day 10. a, b, e, f, i, j, m, n; cortex, c, d, g, h, k, l, o, p; medulla. a, c, e, g, i, k, m, o; HE staining (paraffin sections), b, d, f, h, j, l, n, p; klotho immunohistochemical staining. Arrow: klotho positive tubular cells. d, s: Most of the tubular cells in the medulla were klotho positive. **(b)** Representative immunohistochemical staining for klotho expression in paraffin sections. Klotho staining is seen mainly in distal tubular cells and the collecting duct. The staining was diminished in IRI at day 1, as shown by the frozen sections. a, b; Sham day 1, c, d; IRI day 1, a, c; cortex, b, d; medulla ( $\times 200$ ).



**Fig. 5.** Klotho and TUNEL double staining of renal tubule. Representative immunohistochemical evaluation of klotho expression and apoptotic cells at day 3. TUNEL-positive cells are co-stained with klotho. Arrow: TUNEL-positive cells.

**(a) Kidney****(b) Liver**

**Fig. 6.** Klotho expression after gene transfer with the adenovirus. **(a)** Klotho mRNA and protein expressions in the kidney. Renal klotho mRNA expression in the ad-kl groups was at the same level as that of the ad-LacZ groups. There were no significant differences in protein expression between the ad-kl and ad-LacZ treated groups, as shown by the representative blotting. **(b)** Klotho mRNA and protein expression in the liver. In the ad-kl groups, hepatic klotho gene expression was significantly increased, by more than 500-fold as compared with the ad-LacZ groups. Remarkable expression of the klotho protein was observed in the ad-kl groups as compared with the ad-LacZ treated groups, as shown by the representative blotting.

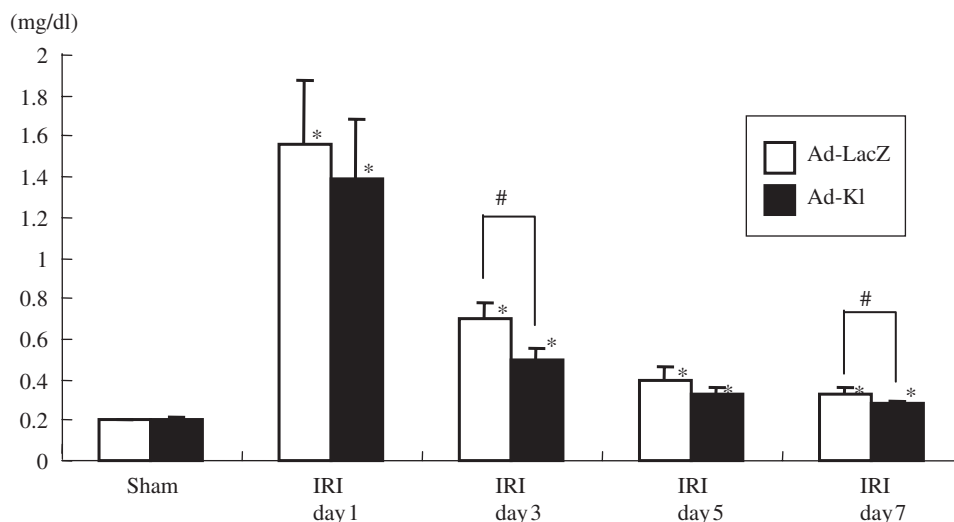


**Fig. 7.** Time course of plasma concentrations of creatinine. Creatinine was significantly reduced in the ad-kl IRI day 3 group as compared with the ad-LacZ IRI day 3 group. Data are given as means  $\pm$  SD. \* $P < 0.01$  compared with the sham-operated group and # $P < 0.05$  compared with the ad-LacZ IRI group. ( $n = 4$  to 5 for each group.)

klotho mRNA and protein expression were confirmed. Hepatic klotho mRNA and protein expressions were significantly increased in the ad-kl groups 3 and 6 days after adenovirus injection (day 3: Figure 6b, day 6: data not shown). However, renal klotho mRNA and protein expressions in ad-kl groups were the same as those of the ad-LacZ groups (day 3: Figure 6a, day 6: data not shown).

Although ad-kl injection did not affect klotho expression in the kidney, elevation of PCR was slightly but significantly blunted in ad-kl rats as compared

with ad-LacZ rats with IRI day 3, 7 (ad-kl day 3 IRI;  $0.50 \pm 0.05$  mg/dl vs ad-LacZ day 3 IRI;  $0.70 \pm 0.08$  mg/dl,  $P < 0.05$ ) (Figure 7).

Renal histological damage was more severe in the ad-LacZ IRI group than in the ad-kl IRI group (Figure 8b). Tubular dilatations in the cortex and protein cast formation in the medulla were particularly severe. As to the ATN score, the ad-kl IRI group showed significant protection from IRI (ad-kl IRI;  $2.42 \pm 0.88$  vs ad-LacZ IRI;  $4.35 \pm 0.43$ ,  $P < 0.005$ ) (Figure 9a).

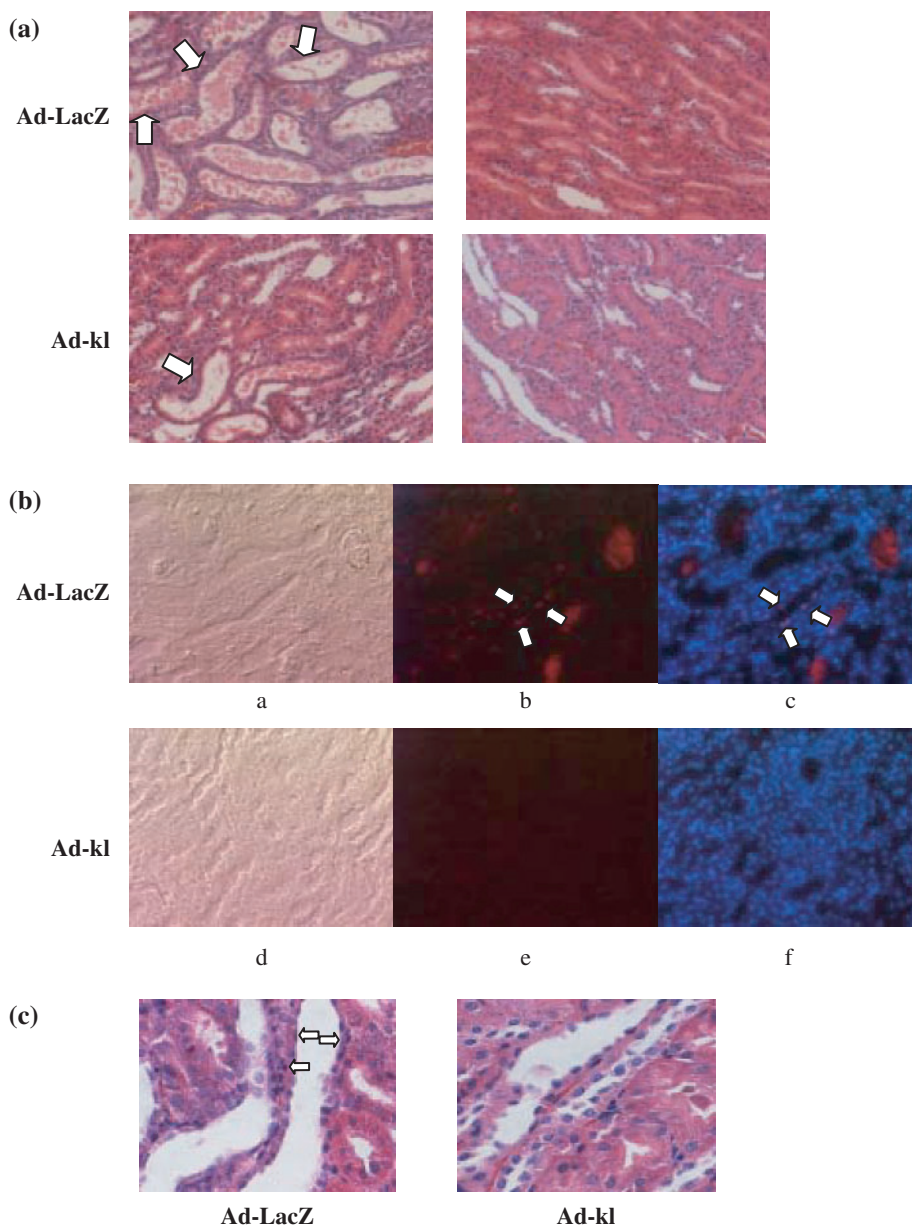


**Fig. 8.** Histological changes after ad-kl treatment. (a) Representative HE staining of renal tubular cells at postoperative day 3 ( $\times 100$ ). Tubular damage in the kidney was attenuated in the ad-kl IRI group as compared with the ad-LacZ IRI group. Arrow; cast formation and tubule dilatation. a, b; Ad-LacZ, c, d; Ad-kl, a, c; IRI, b, d; sham. (b) Representative TUNEL and DAPI staining of renal tubular cells at postoperative day 3. In contrast to the ad-LacZ IRI group, few TUNEL positive cells were observed in the kidney in the ad-kl IRI group. Arrow; apoptotic cells. a–c; Ad-LacZ IRI, d–f; Ad-kl IRI, a, d; phase, b, e; TUNEL, c, f; TUNEL+DAPI (merge). (c) Representative HE staining of renal tubular cells at postoperative day 3 ( $\times 400$ ). In contrast to the ad-LacZ IRI group, few apoptosis cells were observed in the kidney in the ad-kl IRI group. Arrow; apoptotic cells.

We next investigated whether ad-kl administration had any effects on the apoptotic process. Ad-kl administration significantly reduced the number of TUNEL-positive cells in the renal IRI (Figure 8b). There were apoptosis cells in the ad-kl IRI group in HE staining (Figure 8c). There were fewer TUNEL-positive cells in the ad-kl and LacZ sham groups than in the ad-kl and LacZ IRI groups. Moreover, the ad-kl IRI group had fewer TUNEL-positive cells than the ad-LacZ IRI group 3 days after the operation

(ad-kl IRI;  $0.57 \pm 0.23$  vs ad-LacZ IRI;  $2.46 \pm 1.21$ ,  $P < 0.005$ ) (Figure 9b).

## Discussion

We showed IRI to reduce renal klotho gene and protein expressions in this study. In addition, adenovirus-mediated klotho gene transfer attenuated the elevation of serum creatinine and renal morphological damage.

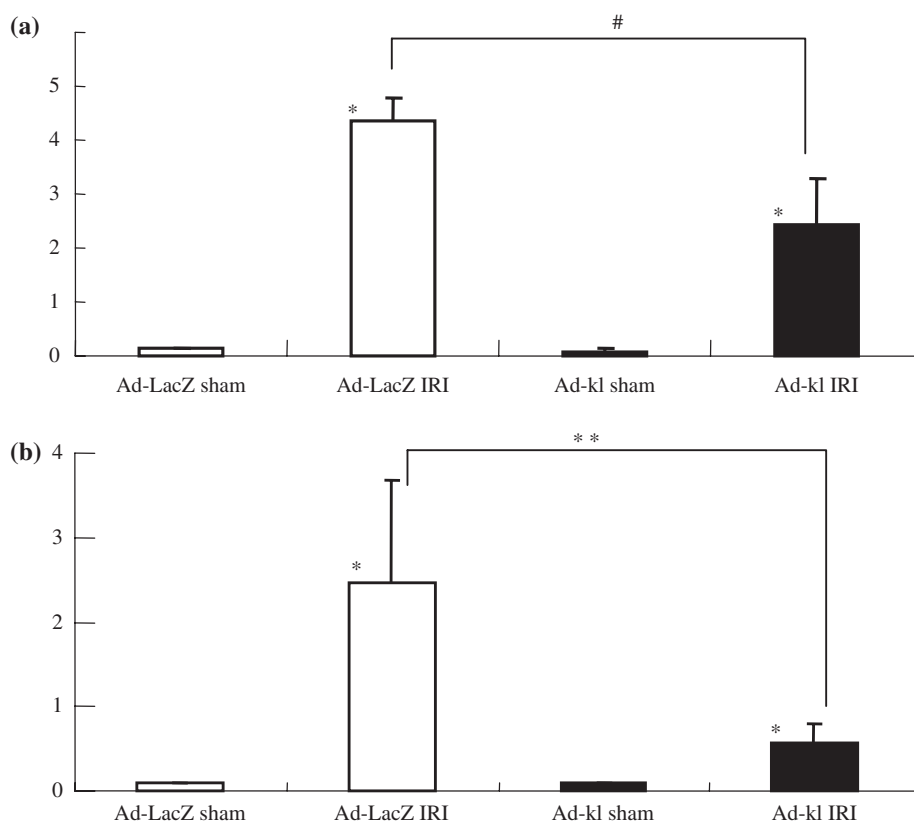


**Fig. 9.** Semi-quantitative analysis of ad-kl treatment. (a) ATN score. The ATN score was significantly attenuated in the ad-kl group in comparison with the ad-LacZ group in day 3 IRI. Data are given as means  $\pm$  SD. \* $P$  < 0.01 compared with the sham-operated group and # $P$  < 0.05 compared with the ad-LacZ IRI group. ( $n$  = 5 to 6 for each group.) (b) Number of apoptotic cells. In the kidneys, the number of TUNEL-positive cells in the ad-kl group was less than that in the ad-LacZ group in day 3 IRI. Data are given as means  $\pm$  SD. \* $P$  < 0.01 compared with the sham-operated group and # $P$  < 0.05 compared with the ad-LacZ IRI group. ( $n$  = 5 to 6 animals in each group.)

These data indicate that klotho plays a crucial role in the pathophysiology of renal IRI.

In previous studies using animal hypertension models, such as the spontaneously hypertensive rat, deoxy corticosterone acetate (DOCA)-salt hypertensive rat and angiotensin II-infused rats [3], downregulation of klotho mRNA in the kidney was found. Not only high blood pressure but also several forms of stress and disease states, such as experimental diabetes [11], chronic renal failure or ageing, reportedly reduce klotho mRNA and protein in the kidney. In addition to the klotho suppression under sustained stress, changes caused by acute stress such as lipopolysaccharide (LPS) loading have been recognized [3]. In this study, we adopted the renal ischemia-reperfusion injury model for observation of klotho expression and then investigated the role of klotho in a typical renal stress model.

The biological properties of klotho protein have not yet been clarified. The phenotype of mice with the mutated klotho gene has been postulated to involve calcification of the arteries, osteoporosis, pulmonary emphysema, dermal atrophy, etc. [1]. Changes in the vasculature were reportedly not only calcification-related, but also associated with endothelial dysfunction [12]. The vasodilatory response to acetylcholine is significantly attenuated in klotho knockout mice, and

moreover, urinary nitric oxide (NO) metabolites are reduced in heterozygous and knockout mice. These data suggest that the klotho protein mediates NO production by the vascular system. Endothelium-dependent relaxation was also attenuated, possibly due to a decrease in NO production by endothelial cells. The same group demonstrated klotho gene delivery to improve endothelial dysfunction in an experimental rat model with multiple atherogenic risk factors [11]. Recently, it was reported that the activity of klotho protein was mediated by cAMP and a NO-cGMP dependent pathway with a second messenger [12]. However, no other information on the functional properties of klotho proteins has become available.

Investigations of the mechanisms involved in the development of renal dysfunction and injury due to IRI have revealed adhesion molecule expressions and an inflammatory process [13,14], with subsequent production of reactive oxygen species [15] and NO, which play important roles in the pathogenesis of IRI [16]. We confirmed, as expected, that klotho expression in tubular cells was initially reduced and then gradually returned to the control level. IRI is likely to be responsible for severe damage to renal tissue, resulting in non-specific downregulation of several genes. However, we demonstrated in a previous study that



there is an apparent alteration of gene expression levels in the IRI kidney as assessed using a microarray system, which could not be explained solely by the degradation of a variety of proteins. mRNA expression levels were quantitated based on standard genes by the real time PCR method. Thus, downregulation of the *klotho* gene was specific under the stressful conditions employed herein. However, the physiological role of *klotho* in this stress state is unclear, and some of the protective or anti-stress functions of *klotho* may, as noted in previous reports, involve the vascular and other systems [11,12].

We thus used a recombinant adenovirus expressing the membrane form of the mouse *klotho* gene to clarify and examine its role in the amelioration of IRI. Exogenous expressions of *klotho* mRNA and protein were detected in the liver at least 6 days after recombinant adenovirus treatment, but renal expressions showed no statistically significant changes. Recent studies found the *klotho* transgene to be efficiently expressed in the liver, but not in the kidneys, brain, spleen, heart, or aorta [3,10]. Thus, our results are consistent with those of previous studies. As to kidney function, the PCr elevation was significantly attenuated in the ad-kl IRI group as compared with the ad-LacZ IRI group. Although the improvement of PCr was minimal, it is noteworthy that the *klotho* played a protective role against the renal IRI. The precise mechanisms by which *klotho* expression exerts these renal protective and other beneficial effects in the IRI model were not clarified in this study. Attenuation of the process leading to cell death or apoptosis, i.e. reducing the number of TUNEL-positive cells or tissue damage (represented by the ATN score), is a possibility raised by our results. In addition, in our *in vitro* preliminary study, we observed that ad-kl transfection of a cultured collecting cell line prevented cell death and apoptosis in response to oxidant stress (manuscript in preparation). Overall, these data suggest that *klotho* expression attenuates tissue damage in the IRI model. Although numerous findings support a role for *klotho* as an active humoral substance, no direct evidence is currently available. In the future, measurement of plasma levels or receptor identification will reveal the precise function of *klotho* protein under physiological and pathophysiological conditions. The *klotho* gene and its protein expression were localized in the liver, but secreted protein plasma levels are not currently measurable and could reasonably be expected to affect remote organs or tissues [2,3]. This effect may explain the following issue. It is well known that IRI in the kidney mainly affects proximal tubules [17], such that the reduced damage observed in the proximal tubule in ad-kl treated rats may be due to the humoral effects of *klotho* protein expressed in the liver. Another possibility is that *klotho* expression in the distal tubule, as confirmed by immunohistochemistry, may function as a hormone protecting proximal tubule cells. Therefore, the beneficial effects of *klotho* may be attributable to hormonal regulation. The direct effect of specific ad-kl induced renal overexpression of the *klotho* gene would

reveal the biological properties of *klotho* protein in the kidney. However, we presently face technical problems in establishing a kidney-specific adenovirus effect. It is well known that systemic adenovirus therapy for renal disease is greatly hampered by the specific structure of the kidney and therapeutic utility is thus limited [18]. However, several investigators have suggested that this protein may play a role as a humoral factor. If the *klotho* gene is expressed in the liver, biological effects of the *klotho* protein as a humoral factor might reasonably be expected in all organs. Therefore, we assumed that hepatically expressed *klotho* would function in the kidney as a humoral factor.

Previous reports have suggested liver involvement in the pathophysiology of acute renal injury, via mediation of cytokine over-production [19]. The mechanisms of the development of renal dysfunction and injury in IRI have been investigated, and the results have shown adhesion molecule expressions and an inflammatory process to exacerbate tissue damage. There is a possibility that cytokines or other substances derived from the liver worsen or accelerate tissue injury. Although *klotho* expressed in the liver via adenovirus-mediated transfection and over-expressed *klotho* may cancel hepatic involvement, whether *klotho* expressed in the liver exerts any direct effects on the liver itself was not examined in this study. The biological mechanism by which *klotho* diminishes cellular damage has not been clarified. Although co-localization of *klotho* and TUNEL staining was often observed, its significance cannot be explained by the present results (Figure 5). Nevertheless, apoptotic cell numbers with *klotho* gene transfer were observed in this study. In addition, *klotho* transfected cultured cells were resistant to oxidative stress, suggesting regulation of the apoptotic process by *klotho* protein. Although apoptotic tubular cells were detected, overexpression of *klotho* protein effectively reduced the number of apoptotic cells. Oxidative stress has been established to play a crucial role in IRI in rats [17], and the *klotho* protein may be involved in the regulation of anti-oxidative defense mechanisms against renal damage. Another study found that activities of antioxidant enzymes are increased, apoptotic TUNEL-positive cells are detectable, and a potent antioxidant,  $\alpha$ -tocopherol, decreases the number of apoptotic cells in the *klotho* mutant mouse hippocampus [20]. These results suggest that oxidative stress has a crucial role in the age-associated cognition impairment in *klotho* mutant mice, and that *klotho* protein may be involved in the regulation of antioxidative defence. It would be ideal to perform these experiments examining the role of *klotho* protein in *klotho* knockout mice. However, *klotho* knockout mice are so susceptible to stress that IRI is not feasible. Furthermore, knock-out mice are commercially available. Thus, we employed adenovirus-mediated overexpression of *klotho* protein in the IRI rat as our experimental model.

Downregulation of *klotho* expression may be involved in the pathophysiology of IRI associated with the induction of tubular cell apoptosis. Responses

related to renal IRI, such as apoptosis, inflammation, cell differentiation or proliferation, have been clarified using a mass screening technique, namely, cDNA array. Thus, analysing the relationship between klotho and altered gene expressions may reveal the precise role of klotho in renal IRI [7]. Moreover, the induction of klotho mRNA and protein by adenovirus gene transfer raises the novel therapeutic possibility of ameliorating IRI in the kidney. Therefore, application of this gene transfer strategy may have a protective effect in acute renal failure.

*Acknowledgements.* K. Tsuchiya is supported by a Grant-in-aid (C) from the Japanese government. We thank Mayuko Tsuboi and Atsuko Teraoka for their technical assistance.

*Conflict of interest statement.* None declared.

## References

1. Kuro-o M, Matsumura Y, Aizawa H *et al.* Mutation of the mouse klotho gene leads to a syndrome resembling aging. *Nature* 1997; 390: 45–51
2. Shiraki-Iida T, Aizawa H, Matsumura Y. Structure of the mouse klotho gene and its two transcripts encoding membrane and secreted protein. *FEBS Lett* 1998; 424: 6–10
3. Mitani H, Ishizuka N, Aizawa T *et al.* *In vivo* klotho gene transfer ameliorates angiotensin II-induced renal damage. *Hypertension* 2002; 39: 838–843
4. Koh N, Fujimori T, Nishiguchi S *et al.* Severely reduced production of klotho in human chronic renal failure kidney. *Biochem Biophys Res Commun* 2001; 280: 1015–1020
5. Lloberas N, Torras J, Herrero-Fresneda I *et al.* Postischemic renal oxidative stress induces inflammatory response through PAF and oxidized phospholipids. Prevention by antioxidant treatment. *FASEB J* 2002; 16: 908–910
6. Padanilam BJ. Cell death induced by acute renal injury: a perspective on the contributions of apoptosis and necrosis. *Am J Physiol Renal Physiol* 2003; 284: F608–F627
7. Yoshida T, Tang SS, Hsiao LL *et al.* Global analysis of gene expression in renal ischemia-reperfusion in the mouse. *Biochem Biophys Res Commun* 2002; 291: 787–794
8. Kato Y, Arakawa E, Kinoshita S *et al.* Establishment of the anti-klotho monoclonal antibodies and detection of klotho protein in kidneys. *Biochem Biophys Res Commun* 2001; 267: 597–602
9. Melnikov VY, Afaubel S, *et al.* Neutrophil-independent mechanisms of caspase-1- and IL-18-mediated ischaemic acute tubular necrosis in mice. *J Clin Invest* 2002; 110: 1083–1091
10. Shiraki-Iida T, Iida A, Nabeshima Y *et al.* Improvement of multiple pathophysiological phenotypes of klotho (kl/kl) mice by adenovirus-mediated expression of the klotho gene. *J Gene Med* 2000; 2: 233–242
11. Saito Y, Nakamura T, Ohyama Y *et al.* *In vivo* klotho gene delivery protects against endothelial dysfunction in multiple risk factor syndrome. *Biochem Biophys Res Commun* 2000; 267: 767–772
12. Yang J, Matsukawa N, Rakugi H *et al.* Upregulation of camp is a new functional signal pathway of Klotho in endothelial cells. *Biochem Biophys Res Commun* 2003; 301: 424–429
13. Rabb H, O'Meara YM, Maderna P *et al.* Leukocytes, cell adhesion molecules and ischaemic acute renal failure. *Kidney Int* 1997; 51: 1463–1468
14. Bonventre JV. Dedifferentiation and proliferation of surviving epithelial cells in acute renal failure. *J Am Soc Nephrol* 2003; 14: S55–S61
15. Yu BP. Cellular defenses against damage from reactive oxygen species. *Physiol Rev* 1994; 74: 139–162
16. Yu L, Gengaro PE, Niederberger M *et al.* Nitric oxide: A mediator in rat tubular hypoxia/reoxygenation injury. *Proc Natl Acad Sci* 1994; 91: 1691–1695
17. Chien CT, Lee PH, Chen CF *et al.* De novo demonstration and co-localization of free-radical production and apoptosis formation in rat kidney subjected to ischemia/reperfusion. *J Am Soc Nephrol* 2001; 12: 973–982
18. Haviv YS, Takayama K, Nagi PA *et al.* Modulation of renal glomerular disease using remote delivery of adenoviral-encoded soluble type II TGF-beta receptor fusion molecule. *J Gene Med* 2003; 10: 839–851
19. Kielar ML, Jeyarajah DR, Zhou XJ *et al.* Docosahexaenoic acid ameliorates murine ischaemic acute renal failure and prevents increases in mRNA abundance for both TNF-alpha and inducible nitric oxide synthase. *J Am Soc Nephrol* 2003; 2: 389–396
20. Nagai T, Yamada K, Hyoung-Chun Kim *et al.* Cognition impairment in the genetic model of aging klotho gene mutant mice: a role of oxidative stress. *FASEB J* 2002; 17: 50–52

*Received for publication: 20.12.04*

*Accepted in revised form: 30.8.05*